Conformer Interconversion in the Excited State of Constrained Tryptophan Derivatives

Lloyd P. McMahon, Hong-Tao Yu, Marco A. Vela, Guillermo A. Morales, Li Shui, Frank R. Fronczek, Mark L. McLaughlin,* and Mary D. Barkley*,†

Department of Chemistry, Louisiana State University, Baton Rouge, Louisiana 70803-1804

Received: October 21, 1996[⊗]

The conformer model of tryptophan photophysics ascribes the multiple fluorescence lifetimes to ground-state heterogeneity. It is usually assumed that the different conformers do not interconvert in the excited state. Previous studies of two constrained tryptophan derivatives supported this assumption (Colucci, W. J.; Tilstra, L.; Sattler, M. C.; Fronczek, F. R.; Barkley, M. D. *J. Am. Chem. Soc.* **1990**, *112*, 9182−9190; Yu, H.-T.; Vela, M. A.; Fronczek, F. R.; McLaughlin, M. L.; Barkley, M. D. *J. Am. Chem. Soc.* **1995**, *117*, 348−357). Five constrained derivatives have been synthesized and shown to undergo conformer inversion during the lifetime of the excited state. All derivatives have two ground-state conformations as determined by X-ray crystallography, molecular mechanics calculations, and ^{1}H-NMR. Fluorescence lifetime data were fit to single- and double-exponential models and to a reversible two-state excited-state reaction model. 2-Amino-1,2-dihydrocyclopenta[*b*]indole-2-carboxylic acid has a single-exponential decay consistent with conformer inversion much faster than fluorescence decay. 1,2,3,4-Tetrahydrocarbazole-3-carboxylic acid, ethyl 1,2,3,4-tetrahydrocarbazole-3-carboxylate, and their 9-methyl derivatives have double-exponential decays with a minor second component of small positive or negative amplitude. Conformer inversion rates of $\sim 10^7$ s^{-1} were determined by analyzing the fluorescence decay data using the excited-state reaction model. Temperature dependence of the fluorescence lifetimes was measured in H_2O and D_2O, and solvent quenching rates were calculated from the Arrhenius parameters. The carboxylate and carbonyl functional groups appear to have little effect on solvent quenching of indole fluorescence. Model calculations examining the effect of conformer inversion rate on the decay parameters of a biexponential model indicate that the presence of a small amplitude, short lifetime component may be a good predictor of excited-state conformer interconversion of tryptophans in peptides and proteins.

Introduction

The complex photophysics of tryptophan is a double-edged sword in fluorescence studies of protein structure and dynamics.[1,2] The exquisite sensitivity of the indole chromophore to environment makes tryptophan a versatile intrinsic fluorescent probe. However, the factors responsible for the environmental sensitivity must be delineated before the structural information in fluorescence data can be fully realized. Such knowledge is slowly emerging, mainly from studies that examine various photophysical properties of tryptophan and other indole compounds in simple systems.

It is generally accepted that the multiexponential fluorescence decays of the tryptophan zwitterion[3−5] and individual tryptophans in peptides[6,7] are due to ground-state heterogeneity. The conformer model attributes the complicated decay to multiple ground-state conformations with different excited-state lifetimes. The rates of several nonradiative processes may vary among conformational states, resulting in lifetime heterogeneity. However, correlating individual lifetimes with particular conformations and quenching mechanisms has been difficult. The strongest evidence for the conformer model comes from three sources: (1) The fluorescence decays of individual tryptophan conformers measured in supersonic jets are monoexponential.[8,9] (2) The constrained tryptophan derivatives, 3-carboxy-1,2,3,4-tetrahydro-2-carboline, W(1),[10,11] and 3-amino-1,2,3,4-tetrahydrocarbazole-3-carboxylic acid, W(2),[12] have two ground-state conformations and two excited-state lifetimes. Lifetimes were assigned to conformations by correlating the amplitudes of the biexponential fluorescence decay with ground-state populations determined by molecular mechanics and NMR. This task was greatly simplified compared to tryptophan, where six ground-state conformations have been identified by NMR.[13] Association of lifetime with structure suggested plausible quenching mechanisms to explain the lifetime differences between conformers. (3) The decay amplitudes in an oxytocin analog containing tryptophan correlate with the NMR-determined $C^\alpha-C^\beta$ rotamer populations.[7]

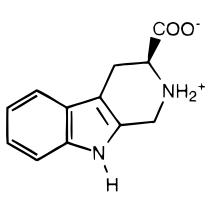

W(1)

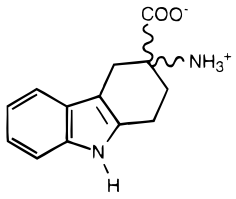

W(2)

The original formulation of the conformer model by Wahl and co-workers considered three scenarios.[14] (1) Conformer interconversion is much slower than the fluorescence time scale. The fluorescence decay is a sum of exponential decays with different excited-state lifetimes and relative amplitudes proportional to ground-state populations. This model is commonly invoked to explain the multiexponential decays of tryptophan-containing compounds.[3,5,7] The two conformers W(1) and W(2) appear to exhibit this behavior.[11,12] (2) Conformer interconversion is much faster than the fluorescence time scale. The fluorescence decay collapses to a single exponential with a decay

† Present address: Department of Chemistry, Case Western Reserve University, 10900 Euclid Ave., Cleveland, OH 44106. E-mail: mdb4@po.cwru.edu.

⊗ Abstract published in *Advance ACS Abstracts,* March 1, 1997.

S1089-5647(96)03273-7 CCC: $14.00

time that depends on conformer lifetimes and interconversion rates. (3) Conformer interconversion is on the fluorescence time scale. The fluorescence decay obeys a kinetic scheme for an excited-state reaction: a sum of exponentials with decay times and preexponentials that depend on conformer lifetimes and interconversion rates.[15] This model was applied by Wahl and co-workers to tryptophanyl diketopiperazines.[14]

There are many examples of adiabatic excited-state reactions: excited-state proton transfer,[16] excimer and exciplex formation,[17] and photoisomerization[18] being the most common. The reactants and products differ, but the underlying kinetic scheme is the same. At least one reactant and one product must be fluorescent to observe an excited-state reaction. Formation of a nonfluorescent product is simply a quenching process. The hallmark of an excited-state reaction is a negative amplitude or rise time in the fluorescence decay. The classical example is the excited-state proton transfer reaction of β-naphthol.[16] Although Wahl and co-workers did not report a negative amplitude for the diketopiperazines, they analyzed their data assuming a two-state excited-state reaction on the fluorescence time scale.[14] Recently, Szabo and co-workers reported a second component with negative amplitude for tryptophan zwitterion at emission wavelengths above 370 nm, but they did not fit their data to an excited-state reaction scheme.[19]

This paper examines conformer interconversion in constrained tryptophan derivatives that have only two ground-state conformations. The compounds selected for study have cyclopentene or cyclohexene rings that invert on time scales from picoseconds to nanoseconds. Their ground-state structures are determined by X-ray crystallography, molecular mechanics calculations, and NMR. The fluorescence decays are analyzed assuming a reversible two-state excited-state reaction for interconversion of the two conformers. Aided by simulation studies, we establish additional criteria for identifying excited-state reactions when the emission spectra of the two species are highly overlapped. Finally, the results provide further information about quenching mechanisms responsible for the lifetime difference between conformers.

Experimental Section

Synthesis. 1,2,3,4-Tetrahydrocarbazole, THC, was purchased from Aldrich, recrystallized from aqueous ethanol, and sublimed under reduced pressure. RP-HPLC (Bondapack C_{18}), 70% methanol: THC was detected by UV (280 nm) as a single peak with a retention time of 12 min. MS: *m*/*z* (relative intensity) 171 (50) M^+, 143 (100). Other compounds were synthesized and purified as described below. All compounds were stored in the freezer protected from light. Solutions were made in H_2O and D_2O (Aldrich, >99% D) containing 0.01 M phosphate buffer at the desired pH.

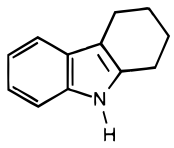

THC

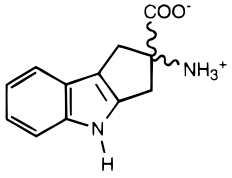

W(2')

2-Amino-1,2-dihydrocyclopenta[*b*]indole-2-carboxylic acid, W(2′), was synthesized in seven steps starting from 2,3-dimethylindole (Supporting Information). The product was purified by ion-exchange chromatography on Amberlite IR-120-plus exchange resin eluted with 0.3 N ammonium hydroxide solution. Solvent removal gave an off-white solid, mp 172 °C; lit. mp 170 °C.[20] IR (KBr): 3405, 1675, 1438, 1202, 1139. ^{1}H NMR (200 MHz, DMSO-d_6): δ 10.94 (s, 1H), 7.72 (b, 2H), 7.31−7.29 (m, 2H), 6.95 (m, 2H), 3.46 (d, J = 16.6 Hz, 1H), 3.26 (d, J = 14.8 Hz, 1H), 2.89 (d, J = 13.8 Hz, 1H), 2.81 (d, J = 14.4 Hz, 1H). ^{13}C NMR (50 MHz, DMSO-d_6): 172.3, 141.1, 140.7, 124.0, 119.8, 118.6, 117.8, 114.5, 111.7, 69.7, 37.1, 36.6. Final purification was done by preparative RP-HPLC (Bondapack C_{18}), gradient: 20−70% B in 25 min; A, water with 0.056% TFA; B, 80% acetonitrile with 0.056% TFA. W(2′) was detected by UV (280 nm) and fluorescence as a single peak with a retention time of 10.5 min. Purity was confirmed by FAB-MS.

Ethyl 1,2,3,4-tetrahydrocarbazole-3-carboxylate, W(1c)E, was prepared by the procedure of Rice and Scott[21] from a commercially available intermediate. A 3.0 g (18 mmol) sample of ethyl 4-oxocyclohexane carboxylate (Aldrich) was refluxed with 1.95 g (18 mmol) of phenylhydrazine in glacial acetic acid (8 mL) under argon for 1.25 h. The solution was allowed to cool and placed in a refrigerator for 3 h. The precipitate was filtered and washed with ice-cold water and 50% alcohol and then treated with decolorizing charcoal in hot benzene. Recrystallization from aqueous ethanol gave colorless needles in 95% yield, mp 93−97 °C; lit. mp 94.5−96 °C.[21] Anal. ($C_{15}H_{17}NO_2$): C, H, N. RP-HPLC (Bondapack C_{18}), 80% methanol, detected by UV (280 nm) as a single peak with a retention time of 13.4 min. FAB-MS: *m*/*z* (relative intensity) 244 (100) $[M + H]^+$, 170 (30). ^{1}H NMR (400 MHz, ref to TMS in $CDCl_3$): δ 7.8 (br s, NH), 7.5 (d, Ar-H), 7.2 (d, Ar-H), 7.1 (m, 2 Ar-H), 4.2 (q, OCH_2), 3.07 (dd, ^2J(HH) 15.18 Hz, H_B), 2.90 (dd, ^2J(HH) 15.18 Hz, H_A), 2.76−2.84 (m, 2 H-C1 and H-C5), 2.32 (m, H-C6, trans to COOEt), 2.03 (m, H-C6, cis to COOEt), 1.3 (t, CH_3). ^{13}C NMR (ref to TMS in $CDCl_3$): δ 175.5 (COO), 135.9, 132.9, 127.5, 121.3, 119.3, 117.7, 110.4, 108.6, 60.5, 40.3, 25.7, 23.8, 22.3, 14.2.

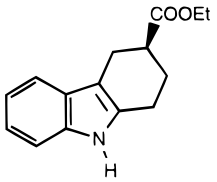

W(1c)E

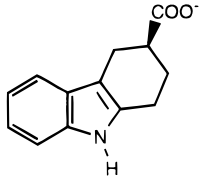

W(1c)

1,2,3,4-Tetrahydrocarbazole-3-carboxylic acid, W(1c), was prepared by hydrolysis of W(1c)E. A solution of 3.0 g (12 mmol) of W(1c)E in 95% ethanol (50 mL) containing 1.5 g (27 mmol) of KOH was refluxed under argon for 3 h. The solvent was evaporated, and the resulting solid residue was taken into 100 mL of water and acidified to pH 2.0 with 6 N HCl. The precipitate was dissolved in 100 mL of ethyl acetate. The aqueous phase was extracted by two 100 mL portions of ethyl acetate. The combined organic phase was dried over sodium sulfate. Evaporation of the solvent gave 2.26 g (86%) of W(1c). The residue was recrystallized three times from aqueous methanol to give a white solid with mp 197−199 °C (decomp); lit. mp 196−198 °C.[21] Anal. ($C_{13}H_{13}NO_2$): C, H, N. RP-HPLC (Bondapack C_{18}), 60% methanol acidified with 0.1% H_3PO_4, pH 2, detected by UV (280 nm) as a single peak with a retention time of 11.8 min. MS: *m*/*z* (relative intensity) 215 (100) M^+, 170 (50). ^{1}H NMR (400 MHz, ref to HDO in D_2O, pD 7): δ 7.58 (d, Ar-H), 7.47 (d, Ar-H), 7.12 (m, 2 Ar-H), 2.98 (dd, ^2J(HH) 15.21 Hz, H_B), 2.72 (dd, ^2J(HH) 15.21 Hz, H_A), 2.77−2.85 (m, 2 H-C1), 2.61 (dddd, H-C5), 2.22 (m, H-C6, trans to COO^-), 1.99 (m, H-C6, cis to COO^-). ^{13}C NMR (ref to TMS in DMSO-d_6): 176.4 (COOH), 135.9, 133.7, 127.0, 120.1, 118.1, 117.1, 110.5, 106.7, 39.5, 25.5, 23.5, 21.8.

Ethyl 9-methyl-1,2,3,4-terahydrocarbazole-3-carboxylate, 9-Me-W(1c)E, was synthesized by a modification of the procedure

for preparing W(1c)E. To a refluxing solution of 0.970 g (5.70 mmol) of 4-(ethoxycarbonyl)-cyclohexanone in glacial acetic acid (2.67 mL) under argon was added dropwise 0.70 g (5.70 mmol) of 1-methyl-1-phenylhydrazine over a 15 min period. The resulting mixture continued to reflux for 1 h. After cooling, the mixture was dissolved in ether, washed with 10% $NaHCO_3$, dried over $MgSO_4$, and evaporated under reduced pressure. A brown oil was obtained (0.64 g, 44%) that eluted as one major peak from GC (30 m DB-5 column, He 30 cm/s, 40−270 °C at 20 °C/min). This product was further purified by RP-HPLC (Bondapack C_{18}), 80% methanol/20% water. ^{1}H NMR (200 MHz, ref to TMS in $CDCl_3$): δ 7.31−7.49 (m, Ar-H), 6.90−7.21 (m, 2 Ar-H), 3.60 (s, N-CH_3) 4.02 (q, OCH_2), 2.59−3.10 (m, 5H), 2.26−2.35 (m, 1H), 1.90−2.17 (m, 1H), 1.11 (t, CH_2CH_3).

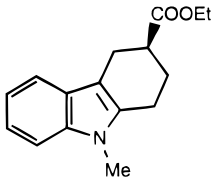

9-Me-W(1c)E

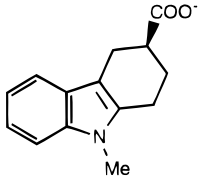

9-Me-W(1c)

9-Methyl-1,2,3,4-tetrahydrocarbazole-3-carboxylic acid, 9-Me-W(1c), was prepared by hydrolysis of 9-Me-W(1c)E. To a solution of 0.425 g (5.06 mmol) of KOH in 95% ethanol (30 mL) was slowly added 1.30 g (5.06 mmol) of 9-Me-W(1c)E under argon. The mixture was refluxed for 1.5 h, and then the solvent was evaporated to dryness. The residue was taken into 40 mL of water and filtered. The filtrate was extracted three times with 40 mL of ethyl acetate. The organic phase was dried over $MgSO_4$, and the solvent was removed under reduced pressure. The residue was taken up in hot methanol, treated with decolorizing charcoal, filtered, and allowed to cool. After several hours, a fine solid separated and was filtered off, washed with water, and recrystallized from benzene (0.708 g, 61%); mp 174−176 °C; lit. mp 174−177 °C.[22] ^{1}H NMR (200 MHz, ref to TMS in $CDCl_3$): δ 10.21 (s, COOH), 7.0−7.59 (m, 4 Ar-H), 3.63 (s, CH_3), 2.12−3.22 (m, 7H).

X-Ray Structure Analysis. Colorless crystals of THC and W(1c)E were grown via slow evaporation of methanol and benzene−hexane, respectively. Intensity data were collected by $\omega-2\theta$ scans of variable rate on Enraf-Nonius CAD4 diffractometers using Cu Kα radiation (λ = 1.541 84 Å) for THC and Mo Kα radiation (λ = 0.710 73 Å) for W(1c)E and graphite monochromators. Crystal data: THC; $C_{12}H_{13}N$, MW = 171.2, orthorhombic space group $P2_12_12_1$, a = 6.1219(13) Å, b = 7.9586(10) Å, c = 19.472(2) Å, V = 948.7(4) Å^3, Z = 4, D_c = 1.199 g cm^{-3}, μ(Cu Kα) = 4.99 cm^{-1}, T = 295 K, crystal size 0.10 × 0.25 × 0.50 mm. Two octants of data within 4° < 2θ < 150° were collected. Data reduction included corrections for background, Lorentz, polarization, decay (5.6%, linear), and absorption. Absorption corrections were based on ψ scans, and the minimum relative transmission coefficient was 88.74%. Equivalent data were merged (R_{int} = 0.015) to yield 1953 unique data, of which 1775 had $I > 3\sigma(I)$ and were used in the refinement. Crystal data: W(1c)E; $C_{15}H_{17}NO_2$, MW = 243.3, monoclinic space group $P2_1/c$, a = 10.219(2) Å, b = 7.5103(10) Å, c = 17.527(5) Å, β = 101.67(2)°, V = 1317.4 (5) Å^3, Z = 4, D_c = 1.227 g cm^{-3}, μ(Mo Kα) = 0.76 cm^{-1}, T = 298 K, crystal size 0.25 × 0.38 × 0.45 mm. One quadrant of data within 2° < 2θ < 55° was collected. Data reduction included corrections for background, Lorentz, polarization, and decay (7.4%, linear). Absorption effects were negligible. Equivalent data were merged (R_{int} = 0.020) to yield 3015 unique data, of which 1348 had $I > 1\sigma(I)$ and were used in the refinement.

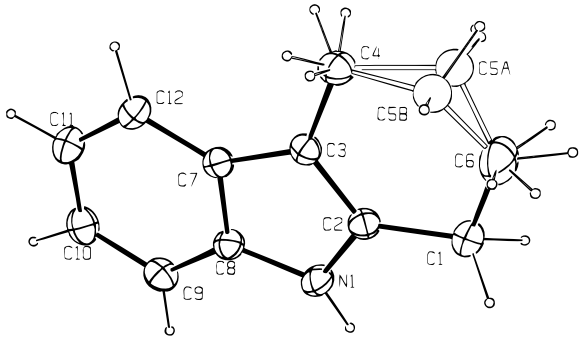

Figure 1. X-ray crystal structure of THC.

TABLE 1: Coordinates and Equivalent Isotropic Thermal Parameters for THC

atom	x	y	z	B_{eq},[a] Å^2
N1	0.7449(3)	−0.0992(2)	0.45653(8)	4.31(3)
C1	0.6730(4)	−0.0157(3)	0.3327(1)	5.21(5)
C2	0.6216(3)	−0.0180(2)	0.40771(9)	3.80(3)
C3	0.4439(3)	0.0540(2)	0.43783(9)	3.50(3)
C4	0.2741(3)	0.1487(3)	0.3981(1)	4.60(4)
C5a	0.2946(6)	0.1039(5)	0.3197(2)	4.87(7)[b]
C5b	0.353(1)	0.1879(7)	0.3277(3)	4.9(1)[c]
C6	0.5077(5)	0.0840(4)	0.2954(1)	8.64(8)
C7	0.4540(3)	0.0153(2)	0.50935(9)	3.48(3)
C8	0.6447(3)	−0.0815(2)	0.51992(9)	3.74(3)
C9	0.7042(4)	−0.1414(3)	0.5843(1)	4.44(4)
C10	0.5711(4)	−0.1042(3)	0.6382(1)	4.91(5)
C11	0.3801(4)	−0.0092(3)	0.6290(1)	5.03(4)
C12	0.3217(3)	0.0521(3)	0.5658(1)	4.45(4)

[a] $B_{eq} = (8\pi^2/3)\sum_i\sum_j U_{ij}a_i^*a_j^*\mathbf{a_i}\cdot\mathbf{a_j}$. [b] C5a is populated 60%. [c] C5b is populated 40%.

The structures were solved by direct methods and refined by full-matrix least-squares based on F with weights $w = \sigma^{-2}(F_o)$, using the Enraf-Nonius SDP programs.[23] Non-hydrogen atoms of THC and W(1c)E were refined anisotropically except C5 of THC, which was disordered into two partially populated positions, C5a and C5b, separated by 0.772(7) Å. The populations of these sites were estimated to be 60% and 40%, respectively, by experiments in which multiplicities were refined. The multiplicities were thereafter fixed at these values, and C5a and C5b were refined isotropically. All hydrogen atoms of THC were refined isotropically except for the partially populated ones on C4, C5a,b, and C6, which were fixed in calculated positions. The N−H hydrogen of W(1c)E was refined isotropically; all others of W(1c)E were fixed. At convergence for THC: R = 0.048, R_w = 0.065, GOF = 2.672 for 146 variables, and the maximum residual electron density was 0.31 e Å^{-3}. The numbering scheme and a perspective view of THC are shown in Figure 1. Final coordinates of THC are listed in Table 1. At convergence for W(1c)E: R = 0.077, R_w = 0.050, GOF = 1.655 for 167 variables, and the maximum residual density was 0.22 e Å^{-3}. The numbering scheme and a perspective view of W(1c)E are shown in Figure 2. Final coordinates of W(1c)E are listed in Table 2.

Molecular Mechanics. Molecular mechanics calculations were done with the MM2 program, modified as described.[11] The dielectric constant of water ϵ = 78.3 was used in the calculations. Starting coordinates for THC and W(1c)E were determined from the crystal structures; coordinates for W(1c) were obtained by replacing the ethyl group in W(1c)E with a hydrogen atom; coordinates for 9-Me-W(1c) and 9-Me-W(1c)E were obtained by replacing the hydrogen on N1 in the crystal structure of the parent compound with a methyl group;

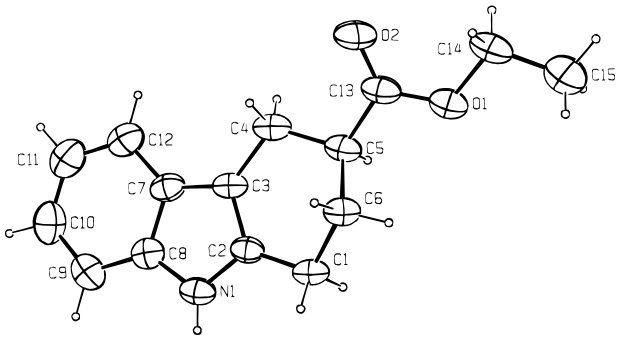

Figure 2. X-ray crystal structure of W(1c)E.

TABLE 2: Coordinates and Equivalent Isotropic Thermal Parameters for W(1c)E

atom	*x*	*y*	*z*	B_{eq},[a] Å^2
O1	0.2891(2)	0.1062(3)	0.7353(1)	7.11(6)
O2	0.0776(2)	0.1482(3)	0.6763(1)	7.75(7)
N1	−0.0193(2)	0.2677(3)	1.0125(1)	5.28(6)
C1	0.1838(3)	0.2711(4)	0.9498(1)	5.09(8)
C2	0.0407(3)	0.2362(4)	0.9506(1)	4.49(7)
C3	−0.0506(3)	0.1733(4)	0.8899(1)	4.74(7)
C4	−0.0190(3)	0.1314(4)	0.8126(2)	5.67(8)
C5	0.1304(3)	0.1307(4)	0.8158(1)	5.52(8)
C6	0.2012(3)	0.2825(4)	0.8652(1)	5.46(8)
C7	−0.1743(3)	0.1623(4)	0.9147(2)	5.14(8)
C8	−0.1528(3)	0.2235(4)	0.9918(2)	5.03(7)
C9	−0.2553(3)	0.2372(5)	1.0333(2)	6.36(9)
C10	−0.3806(3)	0.1855(5)	0.9949(2)	7.6(1)
C11	−0.4044(3)	0.1208(5)	0.9192(2)	7.7(1)
C12	−0.3027(3)	0.1099(5)	0.8785(2)	6.70(9)
C13	0.1603(3)	0.1296(4)	0.7352(2)	5.62(8)
C14	0.3263(3)	0.1026(5)	0.6593(2)	7.2(1)
C15	0.4733(3)	0.0828(7)	0.6723(2)	9.3(1)

[a] $B_{eq} = (8\pi^2/3)\sum_i\sum_j U_{ij} a_i^* a_j^* \mathbf{a_i}\cdot\mathbf{a_j}$.

coordinates for W(2′) were obtained using the MM2 input assist program from Quantum Chemical Program Exchange (Indiana University, No. 543). Minimization of these initial structures yielded the T conformation, which puts the carboxylate in the pseudoequatorial position. Other minimum enthalpy conformational states were explored by driving dihedral angles in the cyclohexene or cyclopentene ring. Torsional barriers for conformer interconversion were obtained by driving the dihedral angle in both directions. Conformer populations were calculated from a Boltzmann distribution at 298 K using the relative enthalpy.

NMR. ^{1}H-NMR spectra were recorded on a Bruker AM400 at room temperature. W(1c) was dissolved in D_2O at pD 7. W(1c)E was not soluble enough in D_2O, so solutions were made in $CDCl_3$ and C_6D_6. Resonances in the cyclohexene ring were assigned by decoupling experiments. For the ABX system (Figure 3), the larger coupling constant was assigned to the trans protons, H_A and H_X, and the smaller coupling constant to the cis protons, H_B and H_X. Coupling constants for the dihedral angle θ between hydrogens were predicted using the substituted ethane model.[11,24]

$$^3J(\theta) = A + B\cos\theta + C\cos 2\theta + \cos[(S_1 + S_4)\cos(\theta - 120) + (S_2 + S_3)\cos(\theta + 120)] \quad (1)$$

where the substituent constants S_i were determined from experimental coupling constants for substituted ethanes:

$$S_i = 4(A - {}^3J) \qquad i = 1, 2, 3, 4 \quad (2)$$

Values of ^3J are H, ethane, 8.0 Hz;[25] COO^-, propionic acid in D_2O at pD 10.05, 7.66 Hz;[26] COOEt, ethyl propionate, 7.60 Hz;[24] C=C, 1-butene, 7.5 Hz;[24] C−C, 2,2-dimethylbutane, 7.56 Hz.[24] Values of $A = 8.0$, $B = -2.7$, and $C = 7.11$ were used.[24]

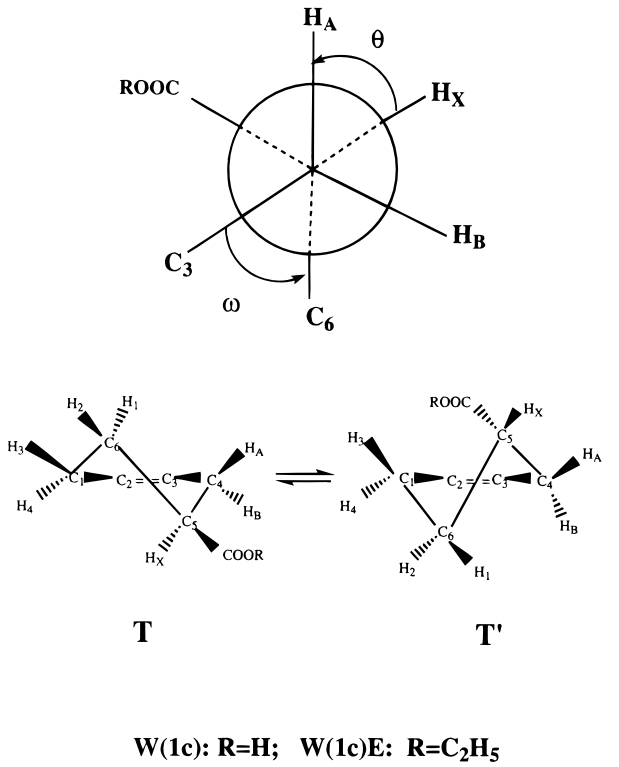

W(1c): R=H; W(1c)E: R=C_2H_5

Figure 3. T and T′ conformers and their Newman projections.

Conformers and populations of W(1c) and W(1c)E were calculated from experimental coupling constants by solving eqs 3,

$$^3J_{MX} = \sum_i P_i {}^3J_{MX}(\omega_i) \quad (3a)$$

$$\sum_i P_i = 1 \quad (3b)$$

where M = A or B and θ in eq 1 is expressed in terms of the torsion angle ω between heavy atoms C3−C4−C5−C6 (Figure 3). MM2 calculations strongly suggest that W(1c) and W(1c)E have only two stable conformers, T and T′. Assuming only two conformers, there are three unknowns: two torsion angles, ω_T and $\omega_{T'}$, and the relative population $P_T = 1 - P_{T'}$. The system of equations is underdetermined with two coupling constants. As done previously for W(1), ω_T for the T conformer was fixed at the MM2 value and eqs 3 were solved for $\omega_{T'}$ and P_T.[11]

Absorbance and Steady-State Fluorescence. Absorbance was measured on an Aviv 118DS spectrophotometer in 1 cm cells. Temperature was regulated at 25 °C by a circulating water bath. Sample absorbance was adjusted to <0.1 at 280 nm for steady-state fluorescence measurements and <0.2 at 295 nm for time-resolved fluorescence measurements.

Steady-state fluorescence measurements were made on an SLM 8000 spectrofluorometer. Temperature was regulated at 25 °C by a circulating water bath. The pK of W(2′) was estimated from fluorescence titration data. Fluorescence quantum yields were measured at 280 nm excitation as described before.[27] Tryptophan in water was used as standard with a quantum yield of 0.14.[28]

Time-Resolved Fluorescence. Fluorescence lifetimes were measured by time-correlated single-photon counting on a Photochemical Research Associates instrument with a picosecond dye laser excitation source as described previously.[27]

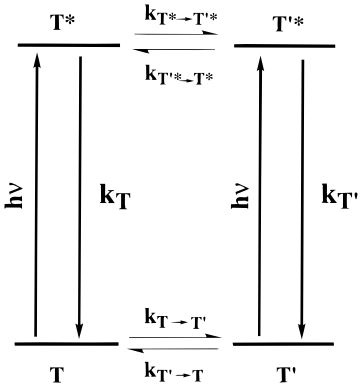

Figure 4. Reversible two-state excited-state reaction model.

Temperature was regulated by a circulating water bath and monitored with an Omega thermistor. Excitation wavelength was 295 nm. Fluorescence decays for sample and reference fluorophore were acquired contemporaneously in 1024 channels of 27 or 54 ps/channel to about 2.5×10^4 counts in the peak. *p*-Terphenyl in ethanol with a single lifetime of 1.06−1.10 ns was the reference fluorophore. For some experiments on W(1c) in H_2O, the instrument was equipped with a cooled Hamamatsu R2809U microchannel plate photomultiplier. The instrumental response was 100 ps fwhm. The data were acquired in 1024 channels of 8.3 ps/channel. An aqueous solution of coffee creamer was used for the instrumental response. Decay curves were deconvolved with a reference decay or lamp profile using the Beechem global program.[29] Time-resolved emission spectra were acquired at 5 or 10 nm intervals from 330 to 430 nm emission wavelength. The data were fitted to a sum of exponentials with amplitudes α_i and lifetimes τ_i. Decay curves acquired at different emission wavelengths were analyzed globally with the lifetimes linked. Radiative k_r and total nonradiative k_{nr} rates were calculated from fluorescence quantum yield Φ and lifetime data.

$$\tau^{-1} = k_r + k_{nr} \tag{4}$$

$$k_r = \Phi/\tau \tag{5}$$

Lifetimes used in eqs 4 and 5 were values from monoexponential fits.

Data sets that gave either a negative or very small positive amplitude for the shorter lifetime species in double-exponential fits were also analyzed assuming a reversible two-state excited-state reaction. In the kinetic scheme of Figure 4, $k_i = \tau_i^{-1}$ are the decay rates of the excited species i = T*, T′* and $k_{i\rightarrow j}$ are the rates of conversion of species i to species j in the excited state. The decay of the total fluorescence intensity $F(\lambda,t)$ at wavelength λ is

$$F(\lambda,t) = S_T(\lambda)\, X_T(t) + S_{T'}(\lambda)\, X_{T'}(t) \tag{6}$$

where $S_i(\lambda)$ are species-associated spectra (SAS) and $X_i(t)$ are fluorescence decays given by eqs 19 in the Appendix. The $S_i(\lambda)$ represent the spectral contours of the individual species i in the absence of species j. The Beechem global program analyzes the fluorescence decay data directly in terms of the rates and SAS. Using the recovered lifetimes and SAS plus the steady-state spectrum $I(\lambda)$, the spectra of the individual species can be determined,

$$I_i(\lambda) = I(\lambda)\, S_i(\lambda)\tau_i / \sum_i S_i(\lambda)\tau_i \tag{7}$$

where $I_i(\lambda)$ is the spectral intensity of species i at wavelength λ.

Fluorescence decays were measured as a function of temperature at one emission wavelength near the emission maximum. Eight or nine decay curves were acquired at temperatures between 3 and 55 °C. Nitrogen gas was flowed through the sample holder to prevent condensation below 20 °C. The temperature dependence of the lifetime is expressed as an Arrhenius factor,

$$\tau^{-1} = k_0 + A \exp(-E^*/RT) \tag{8}$$

where k_0 is the temperature-independent rate, A is the frequency factor, E^* is the activation energy, R is the gas constant, and T is the absolute temperature. The Arrhenius parameters k_0, A, and E^* were linked in global analyses of temperature data in the same solvent.

$$I(t) = \alpha \exp[-\{k_0 + A \exp(-E^*/RT)\}t] \tag{9}$$

Because previous work showed that k_0 and E^* are independent of solvent isotope,[27] their values were also linked between solvents in global analyses of temperature data sets in H_2O and D_2O. The temperature-independent k_{nr}° and temperature-dependent k_{si} nonradiative rates were calculated from the Arrhenius parameters

$$k_{nr}^\circ = k_0 - k_r \tag{10}$$

$$k_{si} = A \exp(-E^*/RT) \tag{11}$$

Results and Discussion

X-ray Structures. The perspective views of THC and W(1c)E are shown in Figures 1 and 2. The conformational averaging seen in the X-ray structure of THC distorts some of the torsion angles in the cyclohexene ring (Table 1). Judging from the large thermal parameters, C6 is probably also disordered, but not resolved into distinct partially populated positions. The 60% populated C5 position of THC, C5a, has some torsion angles reminiscent of a half-chair, while C5b has torsion angles more like a flattened twist-boat. The cyclohexene ring of W(1c)E has a T conformation or half-chair with the ethoxycarbonyl group in a pseudoequatorial position (Table 2). The indole rings of both molecules exhibit only small deviations from planarity. The nine atoms comprising this fragment in THC have an average deviation from coplanarity of 0.005 Å, with a maximum of 0.010(2) Å for C11. This fragment in W(1c)E shows slightly larger deviations, with average 0.012 Å and maximum 0.020(4) Å for both C8 and C10. The N−H group of W(1c)E is involved in an intermolecular hydrogen bond of N···O distance 2.910(3) Å with O2 as acceptor. The hydrogen bond is nearly linear, having an N−H···O angle of 166(3)°.

Solution Conformation. The dihedral driver subroutine of the MM2 program was used to search for minimum enthalpy conformations of the constrained tryptophan derivatives. Only two stable conformations were found by driving torsion angles in the partially unsaturated ring: two envelope conformers of the cyclopentene ring or two half-chair conformers of the cyclohexene ring. The T conformation has carboxylate or ethoxycarbonyl in the pseudoequatorial position; the T′ conformation has this functional group in the pseudoaxial position. The T conformation represents the global minimum. The X-ray and MM2 results are in excellent agreement for the torsion angles in the cyclohexene ring of the T conformer of W(1c)E (Table 3). The cyclopentene ring in W(2′) is flatter than the cyclohexene ring in the other constrained derivatives. The T and T′ conformers differ in the distance between the carboxylate group and the indole chromophore. The carboxylate group is

TABLE 3: Torsion Angles of the T Conformer Derived from MM2 and X-ray

	THC		W(1c)E		W(1c)	9-Me-W(1c)	9-Me-W(1c)E	W(2')[b]
torsion angles	X-ray[a]	MM2	X-ray	MM2	MM2	MM2	MM2	MM2
C3−C4−C5−C13			−167.1	−166.2	−171.2	−166.0	−167.3	−147.2
C1−C2−C3−C4	−0.62	0.0	−0.45	0.14	0.07	0.10	0.61	−0.04
C2−C3−C4−C5	17.1(−13.9)	15.7	11.9	13.9	14.1	14.4	14.7	13.5
C3−C4−C5−C6	−37.9(27.5)	−46.3	−41.0	−44.5	−43.9	−44.2	−45.7	
C1−C6−C5−C4	46.0(−28.6)	64.2	60.9	64.5	62.7	62.1	64.7	
C2−C1−C6−C5	−26.6(11.7)	−45.4	−46.6	−47.2	−45.9	−46.0	−46.3	
C3−C2−C1−C6	2.78	14.9	17.9	16.5	15.9	15.8	15.2	

[a] Numbers in parentheses are for the minor conformation. For details see text. [b] The five-membered ring has the same numbering system as the six-membered ring of the cyclohexene derivatives.

TABLE 4: Relative Enthalpies, Populations, and Energy Barriers from MM2 Calculations

	relative enthalpy[a] T′, kcal/mol	P_T,[b] %	$\Delta H^{\ddagger}_{T\rightarrow T}$, kcal/mol	$k_{T\rightarrow T'}$, 10^9 s^{-1} [c]	$k_{T'\rightarrow T}$, 10^9 s^{-1} [c]
THC	0.0	50	4.3	1.7	1.7
W(1c)	0.46	68	5.1	0.43	1.0
W(1c)E	0.50	70	5.0	0.49	1.2
9-Me-W(1c)	0.61	73	4.5	1.2	3.3
9-Me-W(1c)E	0.62	74	4.5	1.2	3.3
W(2′)	1.47	92	1.7	143	2000

[a] Enthalpy of the T conformer is defined as zero. [b] Calculated from a Boltzmann distribution at 298 K. [c] Estimated from transition-state theory as described in ref 11.

farther away from the indole ring in the T conformer than it is in the T′ conformer. In W(1c), W(1c)E, and their 9-methyl derivatives, the estimated distances between the center of the double bond bridging the benzene and pyrrole rings of indole and the carboxylate carbon atom are about 5.6 Å for the T conformer and 4.2 Å for the T′ conformer. In W(2′), these distances are 5.3 and 4.6 Å, respectively.

THC has two enantiomeric half-chair conformers with the same enthalpies. The methylene groups in the cyclohexene ring, unlike the ammonium or carboxylate groups in the other compounds, have the same distances to the indole ring in both conformations, so that the microenvironments around the indole chromophore are the same. The two conformers should have identical properties except opposite optical rotations. The X-ray structure, in fact, indicates that both conformers are present in the crystal (Figure 2). The T conformation of the cyclohexene ring in W(1c), W(1c)E, and their 9-methyl derivatives is enthalpically favored by about 0.5 kcal/mol, with a population around 70%. It is even more favored (about 1.5 kcal/mol) for the cyclopentene ring of W(2′), having a population of 90%. Barrier heights $\Delta H^{\ddagger}$ for inversion of the cyclohexene ring are in the range 4.3−5.1 kcal/mol for T → T′. These torsional barriers are about 3 kcal/mol higher than the values for the cyclopentene ring of W(2′).

The lower torsional barrier in W(2′) translates to more rapid conformer interconversion. Rates for conformer inversion were estimated from transition-state theory,

$$k_{T\rightarrow T'} = \kappa(kT/h)\exp(-\Delta G^{\ddagger}/RT) \qquad (12)$$

assuming that $\kappa = 0.4$ and $\Delta G^{\ddagger} = \Delta H^{\ddagger}$.[11] The conformer inversion rates of $10^{11}-10^{12}$ s^{-1} for W(2′) are 2−3 orders of magnitude faster than the rates of 10^9 s^{-1} for W(1c), W(1c)E, and their 9-methyl derivatives (Table 4). Because of weakening of the C2−C3 double bond in excited indole plus hydrogen-bonding interactions with solvent not accounted for in MM2, these rates should be regarded as upper limits.[11]

The conformation of the cyclohexene rings of W(1c) and W(1c)E was also determined by ^{1}H-NMR. Two coupling constants were measured in the ABX system (Figure 3; Table 5). The torsion angle ω_T for the T conformer was fixed at the MM2 value, and the torsion angle $\omega_{T'}$ for the T′ conformer and relative populations were determined from eqs 3. The NMR values of $\omega_{T'} = 59°$ and $P_T = 67\%$ for W(1c) are close to the MM2 values of 48° and 68%, respectively. W(1c)E was not sufficiently soluble in water, so NMR experiments were done in benzene and chloroform. Fixing ω_T at the MM2 value, torsion angles $\omega_{T'}$ of 63° and 56° were obtained in benzene and chloroform, respectively. These values are somewhat larger than the 46° calculated by MM2 using the dielectric constant of water. The relative populations are 64% in benzene and 78% in chloroform compared to 73% by MM2. The conformational analyses by MM2 and NMR are in reasonable agreement. The torsion angle appears to be larger in the T′ conformation than the T conformation, suggesting a more puckered ring in the T′ conformer.

TABLE 5: Torsion Angles and Populations Determined by ^{1}H-NMR

	W(1c), D_2O at pD 7		W(1c)E, C_6D_6		W(1c)E, $CDCl_3$	
	NMR	MM2	NMR	MM2	NMR	MM2
J_{AX}, Hz	10.60		9.05		10.02	
J_{BX}, Hz	5.10		6.28		5.22	
ω_T, deg	−44	−44	−45	−45	−45	−45
$\omega_{T'}$, deg	59	48	63	46	56	46
P_T, %	67	68	64	73	78	73

Absorbance and Steady-State Fluorescence. The absorption spectra of THC, W(1c), and W(1c)E at pH 7.0 have a smooth peak at 280 nm and a shoulder at 289 nm. These spectra are less structured than the spectra of tryptophan and W(1)[10] and are slightly red-shifted compared to tryptophan, with a tail of 5% of the maximum absorbance at about 315 nm. For tryptophan the tail is at about 305 nm. The absorption spectra of the 9-methyl derivatives, 9-Me-W(1c) and 9-Me-W(1c)E, are similar to the spectra of THC, W(1c), and W(1c)E, but the tail extends farther to the red. The absorption spectrum of W(2′) is more structured and blue-shifted about 4 nm compared to the spectra of the cyclohexene compounds with maxima at 276 and 285 nm and a shoulder at 290.

Fluorescence emission maxima and quantum yields are given in Table 6. Among the constrained tryptophan derivatives examined so far, the emission maxima of THC, W(1c), and W(1c)E are farthest to the red. As in the case of W(1), methylation of the indole nitrogen shifts the maximum another 12−13 nm to the red. The red shift in fluorescence emission maxima parallels the shift in the tail of the absorption spectra in the order 9-Me-W(1c) ≈ 9-Me-W(1c)E > W(1c) ≈ W(1c)E > THC. The emission maxima of the W(2′) zwitterion and anion, which restricts C^{α} of tryptophan in a five-membered ring, are almost the same as the maxima of the corresponding derivative with a six-membered ring, W(2).[12] Both are shifted about 10 nm to the red relative to tryptophan.

The fluorescence quantum yields for THC, W(1c), and W(1c)E are similar, with values of 0.12−0.18 in H_2O and 0.25−0.31 in D_2O, indicating that the carboxylate and ethoxycarbonyl

TABLE 6: Steady-State Fluorescence Data in H_2O and D_2O at 25 °C[a]

	λ_{max}, nm	Φ	k_r, 10^7 s^{-1}	k_{nr}, 10^7 s^{-1}
		THC		
pH 7	364	0.12 ± 0.01	3.9 ± 0.3	28.0 ± 0.3
pD 7	364	0.25 ± 0.02	3.9 ± 0.3	12.0 ± 0.3
		W(1c)		
pH 7	367	0.14 ± 0.02	3.9 ± 0.5	24.0 ± 0.5
pD 7	368	0.27 ± 0.03	3.8 ± 0.4	10.0 ± 0.4
		W(1c)E		
pH 7	365	0.18 ± 0.02	4.6 ± 0.5	21.0 ± 0.5
pD 7	365	0.31 ± 0.02	4.4 ± 0.3	9.9 ± 0.3
		9-Me-W(1c)		
pH 7	380	0.34	3.9	8.2
pD 7	380	0.52	4.0	3.7
		9-Me-W(1c)E		
pH 7	378	0.39	4.6	7.4
pD 7	378	0.56	4.6	3.6
		W(2′)		
pH 7	360	0.26	6.1	17
pD 7	360	0.40	5.6	8.3
pH 11	370	0.16	4.8	25
pD 11	370	0.29	4.4	11

[a] Values with standard deviation are from 3−5 experiments. k_r and k_{nr} calculated using lifetimes of single-exponential fits from Table 7.

substituent have only a small effect. The ratios of the quantum yield in D_2O and H_2O are rather large, 1.6−2.1, approaching the ratios of 2.2 for 2-methylindole[30] and 2.4 for 2,3-dimethylindole.[31] Quantum yields of the 9-methyl derivatives are about twice those of the parent compounds. The W(2′) zwitterion has a lower quantum yield than the W(1)[27] and W(2)[12] zwitterions. Upon deprotonation of the ammonium group, the quantum yield of W(2′) decreases as it does in W(1) and W(2). The p*K* of the ammonium group of W(2′) estimated from the pH dependence of the fluorescence intensity was 9.0 ± 0.2.

Time-Resolved Fluorescence. Fluorescence decays were measured in H_2O and D_2O at 25 °C. Time-resolved emission spectral data were acquired at 5 or 10 nm intervals between 330 and 430 nm emission wavelength and were deconvolved in global analyses (Table 7). The fluorescence decay of THC gives a good fit to a single-exponential function with a lifetime of 3.1 ns in H_2O and 6.4 ns in D_2O. The W(2′) zwitterion and anion also have single-exponential decays with lifetimes of 4.3 and 3.2 ns, respectively, in H_2O and 7.2 and 6.6 ns in D_2O. Double-exponential fits to these data improve the global reduced chi-squared χ_r^2 and the autocorrelation function of the weighted residuals very little, if at all. W(1c) and W(1c)E in H_2O have apparent single-exponential decays with lifetimes of 3.6 and 3.9 ns, respectively. A double-exponential fit returned two components of similar lifetime for W(1c) and a second component of 40 ps lifetime for W(1c)E with no significant improvement in χ_r^2 or the autocorrelation function. However, in D_2O the double-exponential fits consistently gave lower χ_r^2 values and more random autocorrelation functions. For W(1c)E the second component of short lifetime has negative amplitude across the entire emission band; for W(1c) the amplitude fluctuates between negative and positive values. The amplitudes for the shorter lifetime component are uniformly small, with magnitudes ≤ 11%. To resolve two components for W(1c) in H_2O, another set of time-resolved emission spectral data was collected at higher time resolution. The single-exponential fit to W(1c) decays acquired at 8.3 ps/channel is unacceptable with global $\chi_r^2 = 5.6$ and nonrandom autocorrelation function (Figure 5, upper panel). Fitting to a double-exponential function clearly improves the χ_r^2 value and the shape of the autocorrelation function (Figure 5, middle panel). Single-curve analyses of the decay data for different emission wavelengths usually gave a

TABLE 7: Time-Resolved Fluorescence Data in H_2O and D_2O at 25 °C[a]

	α_1 (360 nm)	τ_1, ns	τ_2, ns	χ_r^2
	THC			
pH 7.0		3.12		1.20
pD 7.0		6.41		1.23
	W(1c)			
pH 7.0		3.63		1.33
pH 7.0, 8 ps/channel		3.59		5.58
	0.10	2.44	3.78	1.74
pD 7.0		7.18		1.32
	-0.08[b]	3.39	7.25	1.17
pD 7.0, 7 °C		12.2		1.70
	0.15	9.32	12.5	1.53
	W(1c)E			
pH 7.0		3.86		1.28
	0.05	0.04	3.90	1.25
pD 7.0		6.97		1.32
	−0.10[b]	4.22	6.98	1.19
	9-Me-W(1c)[c]			
pH 7.0		8.61		1.49
	−0.002	0.046	8.60	1.41
pD 7.0		12.87		1.37
	9-Me-W(1c)E[c]			
pH 7.0		8.22		1.45
	0.05	0.053	8.22	1.38
pD 7.0		12.31		1.52
	W(2′)			
pH 7.0		4.29		1.23
pD 7.0		7.20		1.31
pH 11		3.23		1.22
pD 11		6.62		1.44

[a] Eleven to thirteen decay curves at 330−420 nm emission wavelength. [b] α_1 ranges from 0.05 to −0.11 with $\Sigma\alpha_i = 1$. [c] Eleven decay curves at 350−400 nm emission wavelength (5 nm increments).

second short lifetime component with small positive or negative amplitude and χ_r^2 values in the range 1.3−2.2. Global analysis recovers two closely spaced lifetimes of 2.4 and 3.8 ns and small positive amplitude. The failure to recover the expected short lifetime component may be due to systematic error at 8 ps/channel time resolution, as apparent in the nonrandom residuals at early times (Figure 5). The 9-methyl derivatives of W(1c) and W(1c)E have apparent single-exponential decays with longer lifetimes than the parent compounds. Global fits to double-exponential functions recover a second component with about 50 ps lifetime and small positive amplitude with a slight drop in χ_r^2 and little change in the autocorrelation function.

The radiative k_r and nonradiative k_{nr} rates calculated from quantum yield and lifetime data are given in Table 6. The calculation using eqs 4 and 5 ignores the photoionization yield, which is expected to be small, as discussed elsewhere.[12] The radiative rates k_r of all the compounds are independent of solvent isotope. They are about the same for THC, W(1c), W(1c)E, and the 9-methyl compounds, but slightly faster for W(2′). Moreover, k_r is 1.3-fold faster in the W(2′) zwitterion than the anion. This small effect of a protonated amino group has been noted in other tryptophan derivatives.[4,10,12] The nonradiative rates k_{nr} of all the compounds are 2.0−2.4-fold higher in H_2O than D_2O. This indicates that there is at least one isotopically sensitive quenching process, which will be discussed later. The nonradiative rates of THC, W(1c), and W(1c)E are similar and about 3-fold higher than those of the 9-methyl compounds.

Excited-State Conformer Interconversion. While a second component is evident in the decays of W(1c) and W(1c)E, the very small positive or negative amplitudes and short lifetimes recovered from most of the double-exponential analyses are inconsistent with the conformer model 1 outlined in the Introduction. If the double-exponential decay arises from

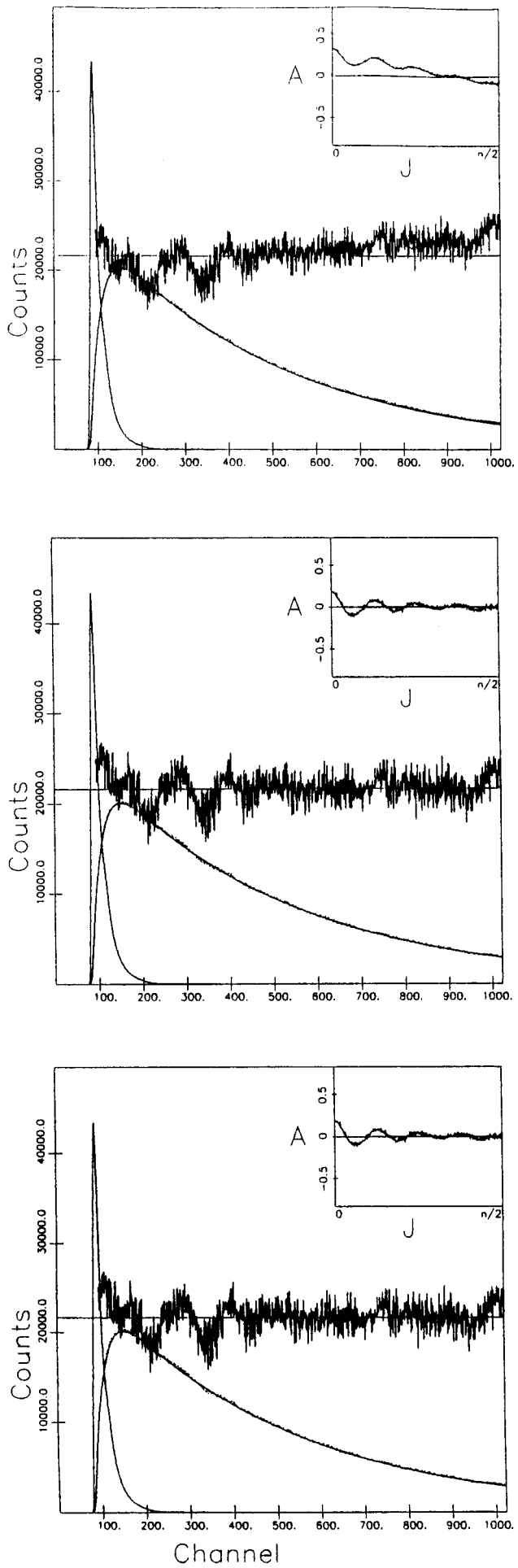

different ground-state conformations that do not interconvert on the fluorescence time scale, then the relative amplitudes of the observed decays should be proportional to the relative populations of conformers. Molecular mechanics calculations and NMR show that all of the compounds having a six-membered ring exist in two conformations with relative ground-state populations of 60−70% for the T conformer and 30−40% for the T′ conformer. The expected values for the relative amplitude of the minor component in double-exponential fits of the excited-state decay are larger than the observed values. Moreover, the presence of negative amplitudes demands a more complex kinetic model. Negative amplitudes in fluorescence decays are diagnostic of excited-state reactions.[32] Given the evidence for an excited-state reaction in the constrained derivatives studied here, what mechanism is responsible? Molecular mechanics calculations and conformer model 3 suggest an answer. The estimated conformer inversion rates for W(1c), W(1c)E, and their 9-methyl derivatives are on the order of 10^9 s^{-1} (Table 4). We consider these values as upper limits, as discussed earlier.[11] Nevertheless, conformer interconversion could occur during the lifetime of the excited state.

With this in mind, the fluorescence decay data for W(1c), W(1c)E, 9-Me-W(1c), and 9-Me-W(1c)E were fit to a reversible two-state excited-state reaction scheme (Figure 4). This system has eight independent variables: two lifetimes, two interconversion rates, two initial concentrations of excited species, and two species-associated spectra. Therefore, it is underdetermined even though some parameters can be fixed or linked in the global analysis. First, assuming that the two conformers have the same extinction coefficient, the initial concentrations of excited species $X_T(0)$ and $X_{T'}(0)$ are fixed at the ground-state populations estimated from MM2. Second, lifetimes τ_T and $\tau_{T'}$ and conformer inversion rates $k_{T^*\rightarrow T'^*}$ and $k_{T'^*\rightarrow T^*}$ are linked in global analyses of decay curves acquired at different emission wavelengths.

The results presented in Table 8 are average values from 4−5 analyses with different starting guesses. The lifetimes are fairly robust. The values are longer, as expected, than those obtained from the double-exponential fit (Table 7). While the uncertainty in the parameters recovered for W(1c) and W(1c)E seems acceptable, errors in one of the interconversion rates are >100% for both 9-methyl derivatives. This suggests that the two-state excited-state reaction model may not be appropriate for 9-Me-W(1c) and 9-Me-W(1c)E. Species-associated emission spectra were calculated for W(1c) and W(1c)E at pD 7.0 by combining time-resolved and steady-state data in eq 7. The species-associated spectra for both species appear to have the same emission maximum (Figure 6).

Excited-state conformer inversion rates for W(1c) appear slightly faster in H_2O than D_2O, although the difference is within experimental error. A deuterium isotope effect on conformer inversion rates noted previously for 3-amino-1,2,3,4-tetrahydrocarbazole, W(1b), was attributed to solvent viscosity.[12] From the ratio of interconversion rates the excited-state equilibrium

Figure 5. Fluorescence decay of W(1c) at pH 7.0, 25 °C. Emission wavelength 365 nm, 8.3 ps/channel. Left curve is lamp profile. Points are sample decay; smooth curve through points is best fit to the following: (upper) single exponential, $\tau = 3.59$ ns; partial $\chi_r^2 = 2.93$, (middle) double exponential, $\alpha_1 = 0.1$, $\tau_1 = 2.44$ ns, $\alpha_2 = 0.9$, $\tau_2 = 3.78$ ns; partial $\chi_r^2 = 1.81$, and (lower) two-state excited-state reaction, $S_T = 0.52 \pm 0.08$, $\tau_T = 3.8 \pm 0.2$ ns, $S_{T'} = 0.48 \pm 0.08$, $\tau_{T'} = 3.7 \pm 0.2$ ns, $k_{T^*\rightarrow T'^*} = 4 \pm 4 \times 10^7$ s^{-1}, $k_{T'^*\rightarrow T^*} = 5 \pm 4 \times 10^7$ s^{-1}; partial $\chi_r^2 = 1.84 \pm 0.02$. Weighted percent residuals and autocorrelation function of the residuals (inset) are also shown. Sinusoidal oscillations in residuals and autocorrelation function appear on the expanded time scale. The oscillations do not affect the lifetime obtained for the monoexponential standard *N*-acetyltryptophanamide.

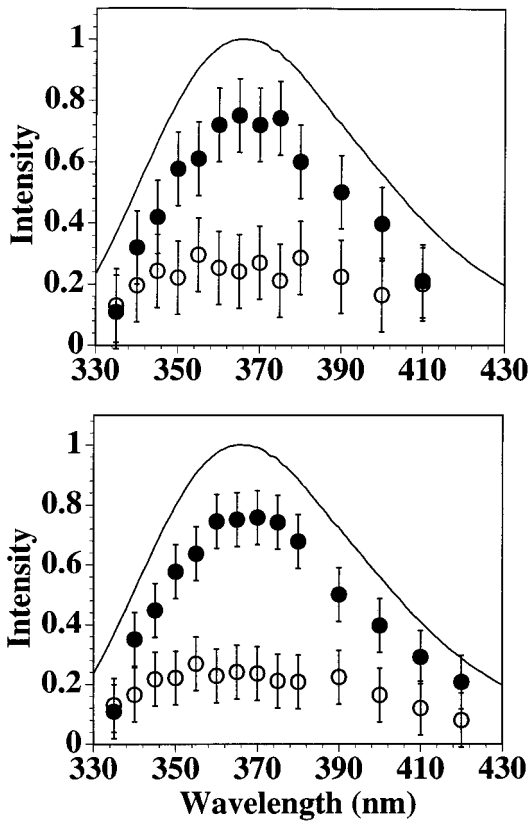

Figure 6. Species-associated emission spectra for (upper) W(1c) and (lower) W(1c)E at pD 7.0, 25 °C: (●) T conformer, (○) T′ conformer, (—) total steady-state emission spectrum. Error bars are standard deviations from 4−5 analyses with different starting guesses.

TABLE 8: Parameters for Excited-State Conformer Interconversion[a]

τ_T, ns	τ_T', ns	$k_{T^*\rightarrow T'^*}$, 10^7 s^{-1}	$k_{T'^*\rightarrow T^*}$, 10^7 s^{-1}	S_T (360 nm)	P_T, %	χ_r^2
W(1c), pH 7.0, 8.3 ps/channel						
3.8 ± 0.2	3.7 ± 0.2	4 ± 4	5 ± 4	0.52 ± 0.08	68	1.78
W(1c), pD 7.0						
8.7 ± 0.7	4.9 ± 0.5	3 ± 1	3.3 ± 0.5	0.7 ± 0.1	68	1.88
W(1c), pD 7.0, 7 °C						
13 ± 1	11 ± 1	0.7 ± 0.2	1.2 ± 0.2	0.71 ± 0.09	68	1.54
W(1c)E, pD 7.0						
9 ± 1	5.0 ± 0.7	7 ± 4	8 ± 6	0.63 ± 0.06	73	1.31
9-Me-W(1c), pH 7.0						
9.5 ± 0.4	6 ± 1	40 ± 50	8 ± 5		70	1.41
9-Me-W(1c)E, pH 7.0						
9 ± 1	6.3 ± 0.9	50 ± 60	16 ± 1		70	1.43

[a] Eleven to thirteen decay curves at 330−420 nm emission wavelength, 25 °C. Errors are standard deviations from 4−5 analyses with different starting guesses.

constant K^* and conformer populations can be estimated.

$$T^* \leftrightarrow T'^* \tag{13a}$$

$$K^* = [T'^*]/[T^*] = k_{T^*\rightarrow T'^*}/k_{T'^*\rightarrow T^*} \tag{13b}$$

The population of the T conformer is about 50% for W(1c) and W(1c)E in the excited state, compared to about 70% in the ground state. However, considering the error in these values, it is not possible to judge whether the ground- and excited-state equilibria are different. The interconversion rates can also be used to calculate the energy barrier for conformer inversion through eq 12. The estimated barrier for W(1c) in D_2O is 6.2 kcal/mol. With a barrier of this magnitude, lowering the temperature from 25 to 7 °C should slow down the interconversion rate 2-fold. The fluorescence decay of W(1c) was measured in D_2O at 7 °C. The fit to a double-exponential decay gives lifetimes of 9.3 and 12.5 ns (Table 7). All amplitudes are positive for the shorter lifetime component in the range from 17 to 9% between 330 and 400 nm. The fit to a two-state excited-state reaction gives interconversion rates that are 3−4-fold slower than the rates at 25 °C (Table 8).

Temperature Dependence of Fluorescence Lifetimes. Previous studies identified two isotopically sensitive temperature-dependent nonradiative processes in indole derivatives: excited-state proton transfer[30,33] and solvent quenching.[12,27] Excited-state proton transfer at neutral pH requires a strong proton donor, such as ammonium. The ammonium group in the W(2′) zwitterion is restricted in the cyclopentene ring and thereby precluded from catalyzing intramolecular proton transfer at aromatic carbons in the indole ring. Excited-state proton transfer has weak temperature dependence in the few cases where it has been determined, with frequency factors of 10^{10} s^{-1} and activation energies of about 4 kcal/mol.[12,34] By contrast, water quenching is strongly temperature dependent, with frequency factors of $10^{15}-10^{17}$ s^{-1} and activation energies of 11−13 kcal/mol. Conformer interconversion is also temperature dependent, with an estimated energy barrier of about 6 kcal/mol in the excited state. As discussed in the Conclusions, in the absence of excited-state proton transfer we can assume that the major temperature-dependent nonradiative pathway is water quenching. Since the lifetimes of the two conformers are similar, we ignore the temperature dependence of conformer inversion and assume a monoexponential fluorescence decay with a single Arrhenius term, as we have done previously.[12,27] Cases where there are two competitive temperature-dependent quenching processes or where the temperature dependence differs in the two conformers would require two Arrhenius terms.[12,35]

Fluorescence decay curves were acquired for the constrained derivatives at various temperatures between 5 and 55 °C in H_2O and D_2O and analyzed according to eq 9. The Arrhenius parameters were assumed to be independent of temperature and were linked in global analyses. In addition, the temperature-independent rate k_0 and activation energy E^* of tryptophan derivatives were previously found to be independent of solvent isotope, so their values were linked in global analyses of data sets from the two solvents. The results are shown in Table 9, along with literature data for several simple indoles. The large frequency factors $A = (6-60) \times 10^{15}$ s^{-1} and activation energies $E^* = 10.8-12.2$ kcal/mol together with a 2.3−2.9-fold deuterium isotope effect on A are characteristic of water quenching.[12,27] Solvent quenching rates k_{si} calculated from eq 11 are given in Table 9. There is a 2−3-fold deuterium isotope effect on k_{si} in all the compounds studied to date.[12,27] As noted previously, methylation of the indole nitrogen and protonation of the amino group slow down water quenching: about 3.5-fold for 9-Me-W(1c) and 9-Me-W(1c)E compared to W(1c) and W(1c)E and about 3-fold for the W(2′) zwitterion compared to the anion.

Temperature-independent processes in indole are fluorescence[36] and intersystem crossing.[37] Internal conversion is not considered an important nonradiative decay channel for indoles, mostly because of the large energy gap between the ground and first excited states. Temperature-independent nonradiative rates k_{nr}° calculated from eq 10 assuming that k_r is independent of temperature are given in Table 9. We presume that k_{nr}° is the intersystem crossing rate for simple indoles, such as THC and the methylindoles. Actually, Klein et al. pointed out that the temperature-independent nonradiative pathway in indole is

TABLE 9: Arrhenius Parameters

compound	solvent[a]	k_0, 10^7 s^{-1}	A, 10^{15} s^{-1}	E^*, kcal/mol	k_{nr}°,[b] 10^7 s^{-1}	k_{si},[c] 10^7 s^{-1}
THC	H_2O	5.7	26	10.9	1.8	26
	D_2O	5.7	9.5	10.9	1.8	9.6
W(1c)	H_2O	6.5	51	11.4	2.6	23
	D_2O	6.5	19	11.4	2.7	8.6
W(1c)E	H_2O	7.5	64	11.6	2.9	20
	D_2O	7.5	25	11.6	3.1	7.5
9-Me-W(1c)	H_2O	5.5	29	11.8	1.6	6.5
	D_2O	5.5	11	11.8	1.5	2.4
9-Me-W(1c)E	H_2O	5.8	28	11.9	1.2	5.3
	D_2O	5.8	12	11.9	1.2	2.2
W(2′)	H_2O, pH 7.0	10.6	31	11.5	4.5	12
	D_2O, pD 7.0	10.6	7.2	11.5	5.0	2.9
	H_2O, pH 11	6.9	18	10.8	2.1	23
	D_2O, pD 11	6.9	6.3	10.8	2.5	8.2
indole	H_2O	12.9	10	10.8	6.4	12
	D_2O	12.5	2.9	10.8	6.0	3.5
N-Me-indole[d]	H_2O	10.3	79	13.1	4.6	2.0
	D_2O	10.3	33	13.1	4.6	0.9
2-Me-indole[e]	H_2O	20.0	82	11.5	13.7	30
3-Me-indole	H_2O	5.8	48	12.2	1.6	5.8
5-Me-indole[e]	H_2O	15.0	3.3	9.7	9.8	25

[a] pH(D) 7.0. [b] Calculated from eq 10. [c] Calculated from eq 11 at 298 K. [d] Reference 27. [e] Reference 40.

intersystem crossing to the triplet state.[37] We expand this case to other indoles with alkyl substituents. Intersystem crossing rates determined this way are in good agreement with values obtained from triplet yields: 7.6×10^7 s^{-1} for indole, 4.0×10^7 s^{-1} for *N*-methylindole, and 2.1×10^7 s^{-1} for 3-methylindole.[35]

Conclusions

A negative amplitude in a multiexponential fluorescence decay is considered the principal indicator of an excited-state reaction, conformer inversion being the present example. A closer look at the kinetic model shows that while a negative amplitude is a sign of conformer inversion during the lifetime of the excited state, lack of a negative amplitude does not mean absence of an excited-state reaction.

For the reversible two-state excited-state reaction depicted in Figure 4, eq 6 for the decay of the total fluorescence intensity, $F(\lambda,t)$, can be rearranged to

$$F(\lambda,t) = [S_T(\lambda)a_1 + S_T(\lambda)b_1]\exp(-\gamma_1 t) + [S_T(\lambda)a_2 + S_T(\lambda)b_2]\exp(-\gamma_2 t) \quad (14)$$

where a_i and b_i are given by eqs 22 and 23, and γ_i is given by eq 20 in the Appendix. The amplitudes recovered from a double-exponential fit are $\alpha_1 = S_T(\lambda)a_1 + S_T(\lambda)b_1$ and $\alpha_2 = S_T(\lambda)a_2 + S_T(\lambda)b_2$ and the decay times are γ_1^{-1} and γ_2^{-1}. The decay times are functions of fluorescence decay and conformer inversion rates; the amplitudes are functions of ground-state populations, fluorescence decay and conformer inversion rates, and emission spectral contours of the individual species. To illustrate how conformer inversion or any excited-state reaction with a fluorescent product influences the recovered parameters, we calculated amplitudes and decay times that would be observed using eq 14 with parameters similar to those recovered in the real examples studied here. Lifetimes, ground-state populations, and SAS were fixed at the following values: $\tau_T = 8$ ns ($k_T = 1.25 \times 10^8$ s^{-1}), $\tau_{T'} = 4$ ns ($k_{T'} = 2.5 \times 10^8$ s^{-1}), $X_T(0) = 0.7$, $X_{T'}(0) = 0.3$, and $S_T = S_{T'} = 0.5$; and conformer inversion rates were varied. Figure 7 plots the calculated decay times γ_1^{-1} and γ_2^{-1} and amplitudes α_1 and α_2 *vs* conformer inversion rate. The results are discussed in terms of the three regimes enumerated in the Introduction.

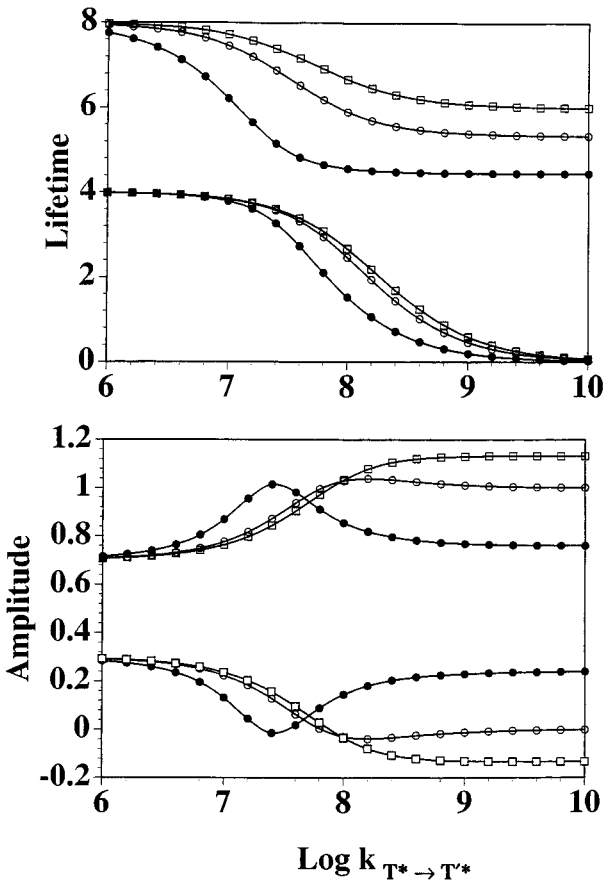

Figure 7. Calculated values of (upper) lifetimes and (lower) amplitudes for a double-exponential decay in the presence of two-state conformer interconversion. $\tau_T = 8$ ns ($k_T = 1.25 \times 10^8$ s^{-1}), $\tau_{T'} = 4$ ns ($k_{T'} = 2.5 \times 10^8$ s^{-1}), $X_T(0) = 0.7$, $X_T(0) = 0.3$, and $S_T = S_{T'} = 0.5$. (○) $k_{T^*\rightarrow T'^*} = k_{T'^*\rightarrow T^*}$, (□) $k_{T^*\rightarrow T'^*} = 0.5k_{T'^*\rightarrow T^*}$, (●) $k_{T^*\rightarrow T'^*} = 4k_{T'^*\rightarrow T^*}$.

(1) Conformer Interconversion Much Slower Than Fluorescence Decay ($k_{T^*\rightarrow T'^*}$, $k_{T'^*\rightarrow T^*} \ll k_T$, $k_{T'}$). Once inversion rates are about an order of magnitude slower than the fluorescence decay, the excited-state reaction is no longer competitive and the model approaches a pure double-exponential decay. Here, γ_1 and γ_2 approach k_T and $k_{T'}$, respectively, and b_1 and a_2 approach zero. Therefore, α_1 and α_2 approach S_1a_1 and S_2b_2, respectively. In W(1c) at 7 °C, the inversion rates $k_{i\rightarrow j}$ are almost 10-fold slower than the fluorescence decay rates k_i. W(1) and W(2) studied previously are other examples of this case.[11,12]

(2) Conformer Interconversion Much Faster Than Fluorescence Decay ($k_{T^*\rightarrow T'^*}$, $k_{T'^*\rightarrow T^*} \gg k_T$, $k_{T'}$). In this case the excited conformers will have time to equilibrate before decaying. As interconversion rates get faster, the double-exponential decay converges to a single-exponential decay with[14]

$$1/\tau = (k_T + Kk_{T'})/(1 + K) \quad (15)$$

where $K = k_{T^*\rightarrow T'^*}/k_{T'^*\rightarrow T^*}$. This lifetime is an average of the two fluorescence decay rates weighted by the excited-state equilibrium constant. W(2′) has a single-exponential decay. Inversion rates $k_{i\rightarrow j}$ of $10^{11}-10^{12}$ s^{-1} predicted from calculated barrier heights (Table 4) are 1000-fold faster than the fluorescence decay rates k_i.

(3) Conformer Interconversion at the Same Rate as Fluorescence Decay. The recovered decay times γ_i^{-1} are generally smaller than the fluorescence lifetimes $\tau_i = k_i^{-1}$ in this region (Figure 7). As conformer inversion rates increase, both γ_1^{-1} and γ_2^{-1} decrease until the shorter of the two becomes

zero and the longer becomes constant. Figure 7 plots the amplitudes $\alpha_1 = S_T(\lambda)a_1 + S_T(\lambda)b_1$ and $\alpha_2 = S_T(\lambda)a_2 + S_T(\lambda)b_2$ *vs* inversion rates for the special case with $S_T(\lambda) = S_{T'}(\lambda) = 0.5$. Other sets of values for $S_i(\lambda)$ generate similar plots (not shown). The amplitude recovered for the shorter decay time is sometimes negative, but it can also be positive or zero. Therefore, the presence of an excited-state reaction cannot be judged solely by whether the analysis generates negative amplitudes. As a consequence of the excited-state reaction, the recovered amplitude for the shorter decay time is always smaller and the recovered amplitude for the longer decay time is always larger than their true values. W(1c), W(1c)E, and their 9-methyl derivatives as well as W(1b)[12] studied previously fall in this intermediate regime. These compounds have roughly 2−6-fold differences between conformer inversion rates $k_{i\rightarrow j}$ and fluorescence decay rates k_i. For W(1c) and W(1c)E, fluorescence decay rates k_i are faster than conformer inversion rates $k_{i\rightarrow j}$. The fluorescence decay in H_2O is sufficiently fast relative to conformer inversion that the excited-state reaction becomes difficult to resolve. By contrast, for W(1b), the conformer inversion rates are faster than the fluorescence decay rates in both H_2O and D_2O, so that the excited-state reaction is a competitive process in both solvents.

An interesting case arises when the two species have the same fluorescence decay rate, $k_T = k_{T'}$, but different ground-state populations and excited-state interconversion rates. The kinetic model predicts a double-exponential decay. W(1c) in H_2O may be an example of this. Although the double-exponential analysis produces two distinct lifetimes, when analyzed assuming an excited-state reaction, the conformer lifetimes are the same within experimental error. Only in cases when $X_{T(0)} = X_{T'(0)}$, and $k_{T'^*\rightarrow T^*} = k_{T^*\rightarrow T'^*}$ as in the case of THC, does it collapse to a single exponential because $a_1 + b_1 = 0$.

The lifetimes of T and T′ conformers in Table 8 differ by ≤1.8-fold, with the T conformer having the longer lifetime. Assuming that the radiative rate k_r is the same in both conformers, the lifetime difference between conformers is due to differences in the nonradiative rate k_{nr}. For tryptophan derivatives incapable of intramolecular excited-state proton transfer, three nonradiative channels are available: intersystem crossing, solvent quenching, and intramolecular excited-state electron transfer. Intersystem crossing rates k_{isc} of simple indoles are not affected by the presence of carbonyl quenchers, such as ethyl acetate.[35] Therefore, we do not expect proximity of the indole ring to carboxylate or ethyl ester groups to change the intersystem crossing rate. Proximity of positively charged amino groups suppresses water quenching.[27] In both W(1b) and W(2) the water quenching rate k_{si} was shown to be slower in the T′ conformer than the T conformer.[12] Table 9 shows a small substituent effect of the carbonyl group on k_{si}, where k_{si} is slightly smaller in W(1c) compared to THC and in the ethyl ester derivatives compared to the carboxylates. Assuming that water quenching would be slower in the conformation with the carbonyl group closer to the indole ring, the effect would be to lengthen the lifetime of the T′ conformer relative to the T conformer. Apparently, differences in k_{si} do not explain the observed lifetime difference, leaving excited-state electron transfer as the most likely quenching mechanism. The lifetime difference between conformers in W(1) and to some extent in W(2) was attributed to electron transfer from excited indole to carboxylate.[11,12] Intermolecular electron transfer to carbonyl quenchers like ethyl acetate is independent of temperature.[35] If we assume that intramolecular electron transfer is also independent of temperature and that W(1c) and W(1c)E have the same intersystem crossing rate as THC, we may estimate the electron transfer rate k_{et} by subtracting k_{nr}° for THC from the values for W(1c) and W(1c)E as $k_{et} = 0.9 \times 10^7\ s^{-1}$ and $1.2 \times 10^7\ s^{-1}$, respectively. A similar estimate of electron transfer rates from data of Kirby and Steiner[38] gives $k_{et} = 1.1 \times 10^7\ s^{-1}$ for indole-3-acetate and $k_{et} = 7.5 \times 10^7\ s^{-1}$ for indole-3-acetic acid ethyl ester. These values for k_{et} are in the same ballpark. However, two inconsistencies are apparent for the cyclohexene derivatives: (1) k_{et} values of $1 \times 10^7\ s^{-1}$ are too small to account for the lifetime difference between conformers and (2) k_{et} values do not increase when carboxylate is replaced by the ester group, which is a stronger electron acceptor. It must also be pointed out that the electron transfer rate included in k_{nr}° is a composite value for both conformers and that the actual quenching rate may be faster in one conformer than the other. A relatively slow electron transfer rate explains the difficulty in resolving a double-exponential decay for W(1c) and W(1c)E in H_2O at 25 °C. As shown in Table 9, the solvent quenching rate k_{si} is by contrast quite high and about 3 times larger in H_2O compared to D_2O. In H_2O solvent quenching dominates the nonradiative rate.

Single tryptophans in proteins and peptides often show multiexponential fluorescence decays. This lifetime heterogeneity arises from multiple ground-state conformations, whose activation energies for interconversion depend on protein structure. Applications of the conformer model to proteins generally assume that the different conformations do not interconvert on the fluorescence time scale. Environmentally sensitive quenching processes that produce lifetime differences among conformers include excited-state proton transfer, excited-state electron transfer, and water quenching. A common practice in interpreting fluorescence decay data for proteins is to inspect the sequence or structure in the vicinity of the tryptophan for functional groups capable of quenching. The present work complicates attempts to associate fluorescence lifetimes with ground-state structure. In the presence of conformer interconversion the decay parameters are no longer simply related to ground-state populations and excited-state lifetimes. Moreover, different conformations involving the same chromophore will have highly overlapped emission spectra, so that the telltale negative amplitude may not be evident. However, the presence of a very short decay time with small amplitude is also a signal of conformer interconversion on the fluorescence time scale. Multiexponential fluorescence decays with a minor short lifetime component have been observed in proteins.[2] In such cases anisotropy experiments to look at local mobility of the tryptophan should prove helpful in interpreting the lifetime data.

Acknowledgment. We thank Dr. Calvin A. Becker for synthesizing 9-Me-W(1c) and 9-Me-W(1c)E. This work was supported by NIH Grant GM42101.

Appendix

The fluorescence decays $X_i(t)$ of the excited species $i = T^*$, T'^* obey the differential equation

$$\dot{X}(t) = \mathbf{T}X(t) \tag{16}$$

where **T** is the transfer matrix

$$\mathbf{T} = \begin{bmatrix} -(k_T + k_{T^*\rightarrow T'^*}) & k_{T'^*\rightarrow T^*} \\ k_{T^*\rightarrow T'^*} & -(k_{T'} + k_{T'^*\rightarrow T^*}) \end{bmatrix} \tag{17}$$

The general solution of eq 16 is

$$X(t) = \mathbf{U}^{-1}X(0)\mathbf{U}\begin{pmatrix} \exp(-\gamma_1 t) \\ \exp(-\gamma_2 t) \end{pmatrix} \tag{18}$$

where γ_i are the eigenvalues of **T,** **U** is the matrix of associated eigenvectors, and $X(0)$ is the vector of initial absorbances of

each species, referred to as bounds in the Beechem global program. The $X_i(0)$ values represent the fraction of incident light absorbed by each species.[3]

The components of eq 18 are

$$X_T(t) = a_1 \exp(-\gamma_1 t) + a_2 \exp(-\gamma_2 t) \quad (19a)$$

$$X_{T'}(t) = b_1 \exp(-\gamma_1 t) + b_2 \exp(-\gamma_2 t) \quad (19b)$$

where γ_i depends on both decay and interconversion rates,

$$\gamma_{1,2} = {}^1/_2[K_1 + K_2 \pm \sqrt{(K_1 - K_2)^2 + 4k_{T^*\rightarrow T'^*}k_{T'^*\rightarrow T^*}}] \quad (20)$$

with

$$K_1 = k_T + k_{T^*\rightarrow T'^*} \qquad K_2 = k_{T'} + k_{T'^*\rightarrow T^*} \quad (21)$$

and where a_i and b_i depend on the rates as well as initial concentrations.

$$a_1 = \frac{X_T(0)(K_1 - \gamma_2) - X_{T'}(0)k_{T^*\rightarrow T'^*}}{\gamma_1 - \gamma_2} \quad (22a)$$

$$a_2 = \frac{-X_T(0)(K_1 - \gamma_1) + X_{T'}(0)k_{T^*\rightarrow T'^*}}{\gamma_1 - \gamma_2} \quad (22b)$$

$$b_1 = \frac{X_{T'}(0)(K_2 - \gamma_2) - X_T(0)k_{T'^*\rightarrow T^*}}{\gamma_1 - \gamma_2} \quad (23a)$$

$$b_2 = \frac{-X_{T'}(0)(K_2 - \gamma_1) + X_T(0)k_{T'^*\rightarrow T^*}}{\gamma_1 - \gamma_2} \quad (23b)$$

Supporting Information Available: Tables of bond distances, bond angles, torsion angles, coordinates for hydrogen atoms, and isotropic thermal parameters for THC and W(1c)E and synthesis of W(2′) (14 pages). This material is contained in many libraries on microfiche, immediately follows this article in the microfilm and CD-ROM versions of the journal, can be downloaded from the ACS via the WWW, and can be ordered from the ACS; see any current masthead page for ordering information.

References and Notes

(1) Creed, D. *Photochem. Photobiol.* **1984**, *39*, 537−562.
(2) Beechem, J. M.; Brand, L. *Annu. Rev. Biochem.* **1985**, *54*, 43−71.
(3) Szabo, A. G.; Rayner, D. M. *J. Am. Chem. Soc.* **1980**, *102*, 554−563.
(4) Chang, M. C.; Petrich, J. W.; McDonald, D. B.; Fleming, G. R. *J. Am. Chem. Soc.* **1983**, *105*, 3819−3824.
(5) Petrich, J. W.; Chang, M. C.; McDonald, D. B.; Fleming, G. R. *J. Am. Chem. Soc.* **1983**, *105*, 3824−3832.
(6) Chen, R. F.; Knutson, J. R.; Ziffer, H.; Porter, D. *Biochemistry* **1991**, *30*, 5184−5195.
(7) Ross, J. B. A.; Wyssbrod, H. R.; Porter, R. A.; Schwartz, G. P.; Michaels, C. A.; Laws, W. R. *Biochemistry* **1992**, *31*, 1585−1594.
(8) Sipior, J.; Sulkes, M.; Auerbach, R.; Boivineau, M. *J. Phys. Chem.* **1987**, *91*, 2016−2018.
(9) Philips, L. A.; Webb, S. P.; Martinez, S. J., III; Fleming, G. R.; Levy, D. H. *J. Am. Chem. Soc.* **1988**, *110*, 1352−1355.
(10) Tilstra, L.; Sattler, M. C.; Cherry, W. R.; Barkley, M. D. *J. Am. Chem. Soc.* **1990**, *112*, 9176−9182.
(11) Colucci, W. J.; Tilstra, L.; Sattler, M. C.; Fronczek, F. R.; Barkley, M. D. *J. Am. Chem. Soc.* **1990**, *112*, 9182−9190.
(12) Yu, H.-T.; Vela, M. A.; Fronczek, F. R.; McLaughlin, M. L.; Barkley, M. D. *J. Am. Chem. Soc.* **1995**, *117*, 348−357.
(13) Dezube, B.; Dobson, C. M.; Teague, C. E. *J. Chem. Soc., Perkin Trans. 2* **1981**, 730−735.
(14) Donzel, B.; Gauduchon, P.; Wahl, P. *J. Am. Chem. Soc.* **1974**, *96*, 801−808.
(15) Mataga, N.; Ottolenghi, M. In *Molecular Association*; Foster, R., Ed.; Academic Press: New York, 1979; Vol. 2; pp 1−78.
(16) Laws, W. R.; Brand, L. *J. Phys. Chem.* **1979**, *83*, 795−802.
(17) Buchberger, E. M.; Mollay, B.; Weixelbaumer, W.-D.; Kauffmann, H. F.; Klopffer, W. *J. Chem. Phys.* **1988**, *89*, 635−652.
(18) Saltiel, J.; Zhang, Y.; Sears, D. F., Jr. *J. Am. Chem. Soc.* **1996**, *118*, 2811−2817.
(19) Willis, K. J.; Szabo, A. G.; Kracjarski, D. T. *Chem. Phys. Lett.* **1991**, *182*, 614−616.
(20) Franceschetti, L.; Garzon-Abureh, A.; Mahmoud, M. R.; Natalina, B.; Pellicciari, R. *Tetrahedron Lett.* **1993**, *34*, 3185−3188.
(21) Rice, L. M.; Scott, K. R. *J. Med. Chem.* **1970**, *13*, 308−311.
(22) Utley, J. H. P.; Yeboah, S. O. *J. Chem. Soc., Perkin Trans. 1* **1978**, *8*, 888−892.
(23) Frenz, B. A. *Enraf-Nonius Structure Determination Package SDP/VAX V3.0*; Enraf-Nonius: Delft, The Netherlands, 1985.
(24) Colucci, W. J.; Jungk, S. J.; Gandour, R. D. *Magn. Reson. Chem.* **1985**, *23*, 335−343.
(25) Lynden-Bell, R. M.; Sheppard, N. *Proc. R. Soc. (London) Ser. A* **1962**, *269*, 385−403.
(26) Colucci, W. J.; Gandour, R. D.; Mooberry, E. A. *J. Am. Chem. Soc.* **1986**, *108*, 7141−7147.
(27) McMahon, L. P.; Colucci, W. J.; McLaughlin, M. L.; Barkley, M. D. *J. Am. Chem. Soc.* **1992**, *114*, 8442−8448.
(28) Chen, R. F. *Anal. Lett.* **1967**, *1*, 35−42.
(29) Beechem, J. M. *Chem. Phys. Lipids* **1989**, *50*, 237−251.
(30) Yu, H.-T.; Colucci, W. J.; McLaughlin, M. L.; Barkley, M. D. *J. Am. Chem. Soc.* **1992**, *114*, 8449−8454.
(31) Ricci, R. W. *Photochem. Photobiol.* **1970**, *12*, 67−75.
(32) Birks, J. B. *Photophysics of Aromatic Molecules*; Wiley-Interscience: London, 1970.
(33) Shizuka, H.; Serizawa, M.; Shimo, T.; Saito, I.; Matsuura, T. *J. Am. Chem. Soc.* **1988**, *110*, 1930−1934.
(34) Shizuka, H.; Serizawa, M.; Kobayashi, H.; Kameta, K.; Sugiyama, H.; Matsuura, T.; Saito, I. *J. Am. Chem. Soc.* **1988**, *110*, 1726−1732.
(35) Chen, Y.; Liu, B.; Yu, H.-T.; Barkley, M. D. *J. Am. Chem. Soc.* **1996**, *118*, 9271−9278.
(36) Robbins, R. J.; Fleming, G. R.; Beddard, G. S.; Robinson, G. W.; Thistlethwaite, P. J.; Woolfe, G. J. *J. Am. Chem. Soc.* **1980**, *102*, 6271−6279.
(37) Klein, R.; Tatischeff, I.; Bazin, M.; Santus, R. *J. Phys. Chem.* **1981**, *85*, 670−677.
(38) Kirby, E. P.; Steiner, R. F. *J. Phys. Chem.* **1970**, *74*, 4480−4490.
(39) Ameloot, M.; Boens, N.; Andriessen, R.; Bergh, V. V.; de Schryver, F. C. D. *J. Phys. Chem.* **1991**, *95*, 2041−2047.
(40) Walker, M. S.; Bednar, T. W.; Lumry, R. In *Molecular Luminescence*; Lim, E. C., Ed.; Benjamin: New York, 1969; pp 135−152.